

This discussion paper is/has been under review for the journal The Cryosphere (TC).
Please refer to the corresponding final paper in TC if available.

A new spatially and temporally variable sigma parameter in degree-day melt modelling of the Greenland Ice Sheet 1870–2013

A. E. Jowett¹, E. Hanna¹, F. Ng¹, P. Huybrechts², and I. Janssens²

¹Department of Geography, University of Sheffield, Sheffield, S10 2TN, UK

²Earth System Sciences and Departement Geografie, Vrije Universiteit, Brussel, Belgium

Received: 27 August 2015 – Accepted: 4 September 2015 – Published: 5 October 2015

Correspondence to: A. E. Jowett (a.jowett@sheffield.ac.uk)

Published by Copernicus Publications on behalf of the European Geosciences Union.

A new spatially and temporally variable sigma parameter in degree-day melt

A. E. Jowett et al.

Title Page

Abstract

Introduction

Conclusions

References

Tables

Figures

⏪

⏩

◀

▶

Back

Close

Full Screen / Esc

Printer-friendly Version

Interactive Discussion



Abstract

The degree-day based method of calculating ice-/snow-melt across the Greenland Ice Sheet (GrIS) commonly includes the temperature parameter sigma (σ) accounting for temperature variability on short (sub-monthly down to hourly) timescales, in order to capture melt in months where the mean temperature is below 0 °C. Sigma is typically assumed to be constant in space and time, with values ranging from ~ 2.5 to 5.5 °C. It is unclear in many cases how these values were derived and little sensitivity analysis or validation has been conducted. Here we determine spatially and temporally varying monthly values of σ for the unique, extended 1870–2013 timescale based on down-scaled, corrected European Centre for Medium-Range Weather Forecasts (ECMWF) Interim (ERA-I) and Twentieth Century Reanalysis (20CR) meteorological reanalysis 2 m air temperatures on a 5 km \times 5 km polar stereographic grid for the GrIS. The resulting monthly σ values reveal a distinct seasonal cycle. The mean summer σ value for the study period is ~ 3.2 °C, around 1 °C lower than the value of 4.2 °C commonly used in the literature. Sigma values for individual summers range from 1.7 to 5.9 °C. Since the summer months dominate the melt calculation, use of the new variable σ parameter would lead to a smaller melt area and a more positive surface mass balance for the GrIS. Validation of our new variable σ dataset shows good agreement with standard deviations calculated from automatic weather station observations across the ice sheet. Trend analysis shows large areas of the ice sheet exhibit statistically significant increasing temperature variability from 1870–2013 in all seasons, with notable exceptions around Summit in spring, and Summit and South Dome in winter. More recently, since 1990, σ has been decreasing, significantly so in the north-west during July. These interannual σ trends reflect climate change and variability processes operating across the ice sheet, several mechanisms of which are briefly discussed.

A new spatially and temporally variable sigma parameter in degree-day melt

A. E. Jowett et al.

Title Page

Abstract

Introduction

Conclusions

References

Tables

Figures



Back

Close

Full Screen / Esc

Printer-friendly Version

Interactive Discussion



1 Introduction

The temperature index melt method exploits the empirical relationship between near-surface air temperature and ablation rate through the calculation of positive degree days (PDDs) (Hock, 2003). Within the PDD calculation, the sigma (σ) parameter is used in the following equation to account for temperature variations due to the diurnal temperature cycle and random weather fluctuations:

$$\sigma = \sqrt{\frac{1}{N} \sum_{i=1}^N (T_i - T_m)^2} \quad (1)$$

where N is the number of temperature observations, T_i is temperature and T_m is the mean temperature. These temperature fluctuations lead to short-term positive excursions that cause melt during months when the average temperature is below 0°C ; therefore σ allows the model to capture melt during these months. Assuming a normal distribution of the fluctuations around T_m , for Δt days we have $\text{PDD} = \Delta t \times \text{EPD}$, where EPD is the expected positive degree given by Eq. (2):

$$\text{EPD} = \frac{1}{\sigma\sqrt{2\pi}} \int_0^\infty T \exp\left[-\frac{(T - T_m)^2}{2\sigma^2}\right] dT \quad (2)$$

or (after evaluating the integral)

$$\text{EPD} = \sigma\beta\left(\frac{T_m}{\sigma}\right) = \sigma\left[\frac{T_m}{\sigma}\phi\left(\frac{T_m}{\sigma}\right) + f\left(\frac{T_m}{\sigma}\right)\right] \quad (3)$$

(Huybrechts and de Wolde, 1999; Janssens and Huybrechts, 2000). Here, the function β involves the standard normal distribution function ϕ and the standard normal density function f . The PDD in a year having the monthly mean temperatures T_m and constant σ is then

A new spatially and temporally variable sigma parameter in degree-day melt

A. E. Jowett et al.

Title Page

Abstract

Introduction

Conclusions

References

Tables

Figures

◀

▶

◀

▶

Back

Close

Full Screen / Esc

Printer-friendly Version

Interactive Discussion



A new spatially and temporally variable sigma parameter in degree-day melt

A. E. Jowett et al.

Title Page

Abstract

Introduction

Conclusions

References

Tables

Figures

◀

▶

◀

▶

Back

Close

Full Screen / Esc

Printer-friendly Version

Interactive Discussion



$$\text{PPD} = \sigma \int \beta \left(\frac{T_m}{\sigma} \right) dt. \quad (4)$$

Equations (1) and (4) allow efficient computation of melt in ice-sheet models by parameterising the effect of diurnal temperature fluctuations and circumventing the need to resolve them. In this paper, we refer to them as the PDD parameterisation, and σ is the temperature-variability parameter.

Numerous GrIS simulations had assumed a constant σ between ~ 2.5 and 5.5°C (e.g. Fausto et al., 2009a; Reeh, 1991; Ritz et al., 1997; Huybrechts and de Wolde, 1999; Janssens and Huybrechts, 2000), with 4.2°C being a typical value (Janssens and Huybrechts, 2000; Hanna et al., 2011). Recently, however, it is realised that the choice of σ can significantly affect melt model output, and that capturing the spatio-temporal variations of σ , notably for the summer months, may improve estimated of GrIS melt (e.g. Lefebre et al., 2002; Fausto et al., 2009a, b). This is even though the PDD method is an empirical index method based on temperature, but in reality surface melt is a function of energy fluxes at the surface (net long wave, net shortwave, turbulent heat fluxes) and these fluxes are not a direct function of surface temperature. The PDD is a quick-and-easy method that is not physically based, but works well when compared to physically-based methods (and is elegant to use as it only has three parameters) (Braithwaite, 1995).

For instance, a sensitivity analysis carried out by Fausto et al. (2009a) showed a 33% increase in the modelled melt area over the GrIS when using a summer σ value of 4.5°C instead of 2.53°C . As an increased summer σ indicates more excursions above 0°C for any given area on the ice sheet, more melt occurs in areas already experiencing melt - in addition to expanding the melt area. Fausto et al. (2009a) derived their lower σ estimate from Eq. (1) based on observed monthly 2 m air temperatures from 1996 to 2006. Similarly, Lefebre et al. (2002) derived July σ values of 2 to 3°C based on 2 m air temperatures from the European Centre for Medium-Range Weather Forecasts (ECMWF) re-analysis at the 20 km grid scale for the year 1991. Lefebre et al. (2002)'s

A new spatially and temporally variable sigma parameter in degree-day melt

A. E. Jowett et al.

Title Page

Abstract

Introduction

Conclusions

References

Tables

Figures

◀

▶

◀

▶

Back

Close

Full Screen / Esc

Printer-friendly Version

Interactive Discussion

results further support the findings of Fausto et al. (2009a), that σ varies spatially and temporally across the GrIS due to the large variations in meteorological and climatic conditions experienced across the ice sheet (Lefebre et al., 2002; Cappelen et al., 2014). It follows that the approach of using a constant σ in the temperature-index parameterisation may be invalid, and that introducing spatial and or temporal variations in σ (e.g. as explored by Fausto et al., 2009a and Lefebre et al., 2002) is fundamentally a better approach.

Consequently, several recent studies have attempted to derive variable σ parameter sets from both automatic weather station (AWS) temperature records and reanalysis temperature products. Fausto et al. (2009b) used Eq. (1) and AWS data from the GrIS to calculate the least squares fit of summer σ from 1996 to 2006 in an observation-based parameterisation. There is a large altitudinal component to the distribution of σ , with values of around 5 °C in the highest elevation regions but only around 2 °C near the periphery of the ice sheet (Fausto et al., 2009b). The authors also identified an annual cycle in σ , with σ values larger in the winter months and smaller during summer (Fausto et al., 2009b; Lefebre et al., 2002). The low summer values were largely attributed to the limiting effects of melt on surface temperatures and therefore near-surface air temperatures during the melt season, which is absent during other months (Fausto et al., 2009b). There is also a larger scatter in σ calculated at lower elevations, which Fausto et al. (2009b) attributed to higher vulnerability to atmospheric variability of the AWS sites located near the coast.

The validation results of Fausto et al. (2009b) show that σ is within 1 °C of the observations at AWS sites, and increasing accuracy with elevation. Despite this agreement, Fausto et al. (2009b) suggest that using just the mean summer σ is not sufficient to model annual ablation. Including an annual σ distribution more realistically depicts real temperature variability; however, Fausto et al. (2009b) stated that the calculation of an “annual distributed cycle” in temperature variations was limited by data availability.

Several more recent studies have sought to address this data availability issue using re-analysis products to calculate σ grids for the GrIS. Sequinot (2013) used ECMWF

calculation of melt within the degree-day calculation. The following two sections discuss our method of calculating the new σ parameter (Sect. 2) and characteristics of the resulting monthly-varying σ (Sect. 3). Section 4 discusses the validation and application of this new parameter, including a discussion of recent temperature variability over the GrlS. The effect of our new σ parameter on the SMB and component outputs from the modified version of the temperature index melt model will be discussed in a separate paper.

2 Datasets and methods

2.1 Pre-processing of temperature data and calculation of σ

For this study, the freely-available gridded 2 m air temperature data from ECMWF ERA-I reanalysis (Dee et al., 2011) spanning 1979–2013 and 20CR meteorological reanalysis version 2 (Compo et al., 2011) spanning 1870–2008 were acquired and subsets extracted covering the Greenland area. These temperatures were then downscaled by a process of bilinear interpolation from the $2^\circ \times 2^\circ$ latitude/longitude grid (20CR) and $80 \text{ km} \times 80 \text{ km}$ (ERA-I) to a $5 \text{ km} \times 5 \text{ km}$ polar stereographic grid. A topographic correction was applied to these downscaled 2 m air temperatures to remove errors associated with differences in orography between the original coarse-resolution reanalysis data and the $5 \text{ km} \times 5 \text{ km}$ grid, following the method of Hanna et al. (2011) that is based on the ice sheet surface DEM of Ekholm (1996). The reanalysis data are available at 6 hourly timesteps for the ERA-I and 3 hourly timesteps for the 20CR.

In order to generate a continuous σ series from 1870–2013 inclusive, some pre-processing of the 2 m air temperatures from both the 20CR and ERA-I was required to merge the two datasets. Following the method of Hanna et al. (2011), the mean monthly difference between the 20CR and ERA-I temperatures were calculated and then added onto the 20CR temperatures as a systematic correction, which did not change the variability in the 20CR but scaled the 20CR 2 m air temperatures to ERA-

A new spatially and temporally variable sigma parameter in degree-day melt

A. E. Jowett et al.

Title Page

Abstract

Introduction

Conclusions

References

Tables

Figures



Back

Close

Full Screen / Esc

Printer-friendly Version

Interactive Discussion



I, correcting for the systematic low-temperature bias when compared to ERA-I (see Fig. 2).

Ferguson and Villarini (2012, 2014) detected the presence of inhomogeneities in 20CR surface air temperature causing step changes in temperature and precipitation between 1940 and 1950 over the United States. These inhomogeneities or breakpoints occur due to factors including an increase in the number of observations used in the reanalysis around this time (Ferguson and Villarini, 2012). The authors noted that these inhomogeneities may vary regionally. We therefore identified and corrected for such inhomogeneities or artificial breakpoints in our 20CR 2 m air temperature. Breakpoint analysis was carried out on the systematically corrected temperature series using the Bai–Perron structural change point test in R version 3.1.1 (Ferguson and Villarini, 2014). The Bai–Perron analysis was first carried out on monthly time series of downscaled, corrected 20CR 2 m air temperatures for each month in turn, to identify any breaks in temperature. The uncertainty estimates for 2 m air temperatures (ensemble spread) were then analysed in the same way. The breakpoints and their 95% confidence intervals were identified in the 2 m air temperature and the spread data and compared to determine the cause of any breaks. If the 95% confidence intervals in both datasets overlap then the cause is determined to be non-climatological and interpreted to be an artificial break in the data that needs correcting, whereas if the respective breakpoint confidence intervals do not overlap the cause is considered climatological (Ferguson and Villarini, 2014). To correct for any artificial breakpoints, the mean 2 m air temperature was calculated for the periods both before and after the breakpoint. The difference between the two means was then added to each year as an inhomogeneity correction in the period before the artificial breakpoint, thus bringing the 2 m air temperatures of the period before the break in line with those afterwards, removing the artificial step change in temperature.

The complete corrected monthly temperature series and 6 hourly (3 hourly) ERA-I (20CR) temperatures were input into Eq. (1) to calculate new σ values. This gave a new spatially and temporally varying 5 km \times 5 km gridded monthly σ series from 1870–2013

A new spatially and temporally variable sigma parameter in degree-day melt

A. E. Jowett et al.

Title Page	
Abstract	Introduction
Conclusions	References
Tables	Figures
◀	▶
◀	▶
Back	Close
Full Screen / Esc	
Printer-friendly Version	
Interactive Discussion	



inclusive. These new σ values provide a more sophisticated and realistic alternative to the conceptually simpler constant σ value, and were interactively fed into the PDD model in Eq. (4).

2.2 Validation of the variable σ parameter

5 In order to investigate how much of an improvement our new temperature variability parameter presents over the constant σ approach, correlation analysis was carried out. The σ fields were correlated with those derived from 2 m air temperature observations of the Danish Meteorological Institute (DMI), GC-Net and Programme for Monitoring of the Greenland Ice Sheet (PROMICE) AWS (Fig. 1), for the time period of available
10 observations at each station (Cappelen et al., 2013; Steffen et al., 1996; Ahlstrøm et al., 2008). The statistical significance of the relationship was used to determine if our new σ values sufficiently capture observed temperature variability, with the 95 % threshold applied as a minimum value for statistical significance. Only stations where the record was two thirds complete were used in the validation.

15 To detect how temperature variability has changed and therefore any potential climate change signals in σ from 1870–2013, trend analysis was carried out at annual, seasonal and monthly timescales. Linear least squares regression for these timescales was conducted for each grid cell to calculate the rate of change per year from 1870–2013 and for the 1990–2013 sub-period of recent strong Arctic amplification (Overland
20 et al., 2014). Standard climatological seasons were used: i.e. spring = March, April, May; summer = June, July, August; autumn = September, October, November; winter = December, January, February. The significance of regional trends was assessed by calculating the p value based on the correlation coefficient of all successive σ values for that grid cell plotted against time and the degrees of freedom (number of time-steps
25 minus two). A p value of 0.05 is defined as the threshold for statistical significance in line with the 95 % significance level used throughout.

A new spatially and temporally variable sigma parameter in degree-day melt

A. E. Jowett et al.

Title Page

Abstract

Introduction

Conclusions

References

Tables

Figures



Back

Close

Full Screen / Esc

Printer-friendly Version

Interactive Discussion



ing June and July the interquartile ranges are narrower, indicating less variability about the mean during these months.

3.3 σ validation

The comparison of modelled (σ calculated from ERA-I and 20CR) and observed (calculated from observed AWS 2 m-air temperature) σ in Fig. 8 shows the strongest correlation with the annual data, which is a highly significant ($p < 0.01$) positive relationship between the observations and modelled σ when averaged over the year. Despite being weaker, the summer and July correlations are still highly significant ($p < 0.01$) positive relationships between the observed and modelled σ . Overall there is statistically significant agreement between the observed and modelled σ calculated from reanalysis data to those data points on the ice sheet for the periods where validation data are available.

There is a systematic bias in the sign of the offset between observed and modelled σ when plotted against elevation (Fig. 9). The new modelled σ parameter overestimates the observed σ in the ablation zone below the equilibrium line altitude (ELA), which lies at ~ 1500 m. There is a shift in the sign of the difference in the accumulation zone where the model parameter underestimates σ compared to the observations. The annual, summer and July correlations in Fig. 9 indicate highly significant negative relationships, with σ decreasing with elevation.

Figure 10 shows weak negative correlations between the difference in observed and modelled σ , and latitude. Despite these correlations being relatively weak compared with those in Fig. 9, the R values indicate all three correlations are highly significant: annual and summer at the 99 % level and July at the 95 % level: this is due to the large number of data points (pixels) on the ice sheet. The trend lines indicate the bias shifts further northwards, with positive differences in the south between 60 and 65° N, shifting to more negative differences further north. This indicates that the new parameter underestimates σ by 0.06 (0.82) °C in the south (north) on average. There is however,

A new spatially and temporally variable sigma parameter in degree-day melt

A. E. Jowett et al.

Title Page

Abstract

Introduction

Conclusions

References

Tables

Figures



Back

Close

Full Screen / Esc

Printer-friendly Version

Interactive Discussion



considerable scatter around the trend lines; therefore this effect is hard to compensate for by further correcting the σ data.

3.4 Trends in σ

All trends in Fig. 11 are positive from 1870–2013, implying that temperature has become more variable over the study period. The largest trends in σ are in the southern and north-western parts of the ice sheet, indicating that temperature has become relatively more variable over time here than anywhere else. The smallest rates of change in σ are consistently found at high elevations in the centre of the ice sheet. This area displays trends ranging from 0.0–0.3 °C decade⁻¹, equivalent to an increased temperature variability of ~ 0.0–4.3 °C over the whole 144 year period. σ is therefore still becoming more variable in the centre but less so than in more peripheral regions. The centre of the ice sheet is also the only region which shows non-statistically significant results for spring and winter, indicating that these weaker trends could occur by chance. In Fig. 11a the annual rate of change in σ for each 5 km × 5 km grid cell is positive from 1870–2013, showing that overall temperature variability has increased. Figure 11b indicates that all p values lie between 0 and 0.006, so we interpret these long-term trends in annual σ to be statistically significant.

The spring plots show a similar spatial pattern in trend to the annual plot, with smaller values around Summit at higher elevations of the ice sheet. The range in values is greater, from ~ 0.7 °C in the centre to ~ 5.8 °C in the north-west periphery of the ice sheet over the whole 144 year period. There is an area around Summit in the centre of the ice sheet where these trends are not significant: p values exceed 0.05 here, indicated by blue, purple and black tones. The rest of the ice sheet shows the trends are statistically significant. The summer trends in Fig. 11g show lower values for the ice sheet as a whole than spring or annual trends. The lowest values are on the west coast and the highest in the south and north-west, indicating areas of weaker and stronger trends respectively, but all are statistically significant (Fig. 11h). Autumn σ trends range from ~ 0.7 °C on the eastern periphery to ~ 6.5 °C in the north-west over the 144 year

A new spatially and temporally variable sigma parameter in degree-day melt

A. E. Jowett et al.

Title Page	
Abstract	Introduction
Conclusions	References
Tables	Figures
◀	▶
◀	▶
Back	Close
Full Screen / Esc	
Printer-friendly Version	
Interactive Discussion	



A new spatially and temporally variable sigma parameter in degree-day melt

A. E. Jowett et al.

Title Page

Abstract

Introduction

Conclusions

References

Tables

Figures

◀

▶

◀

▶

Back

Close

Full Screen / Esc

Printer-friendly Version

Interactive Discussion



2 m air temperatures are fed into the degree-day model for calculating SMB, and are thus essential for better quantifying mass balance. Although the correction process brings 20CR temperatures more in line with ERA-I for the overlap period, there are some discrepancies in absolute values between the fully corrected 20CR and ERA-I series. This suggests that the fully corrected 20CR series in Fig. 3 still does not capture all of the 2 m air temperature variation and underestimates (overestimates) temperatures in 92 (88) out of 180 cases compared to ERA-I. It is unclear why such a large difference of over $\pm 1^\circ\text{C}$ between 20CR and ERA-I occurs in some years, but this could partly be due to the aftermath of climatically-significant volcanic eruptions, e.g. in 1982 and 1983 where 20CR over or under-estimates the volcanic effect on Greenland temperatures compared to ERA-I. The ERA-I reanalysis is assumed to be more accurate than 20CR as the reanalysis product is more sophisticated/higher-resolution and involves the assimilation of far more observations including upper air and satellite data, while the 20CR relies on observed synoptic surface pressures and sea surface temperature boundary conditions prescribed from HadISST1 (Wake et al., 2009; Hanna et al., 2011; Compo et al., 2006, 2011; Dee et al., 2011). The 20CR temperature fluctuations are smaller in magnitude compared to ERA-I, possibly due to the lower spatial resolution of 20CR ($2^\circ \times 2^\circ$) compared to ERA-I ($\sim 0.75 \times 0.75^\circ$), which could lead to artificially small σ values from 20CR, assuming ERA-I to be the more accurate series.

Residual differences after 1979 between the spliced and un-spliced series, when the ERA-I is incorporated into the spliced series, may be attributable to resolution differences present in the original datasets before downscaling as this latter part of the series is not affected by breakpoints. The notable convergence of temperatures after 1930 in Fig. 4 is synchronous with an increasing σ from around 1930. This increase in σ may be partly attributable to more temperature observations being assimilated by 20CR into the model – which may well improve the calculations of both absolute temperature and its variability – with decreasing accuracy and artificially smooth temperature variability inherent before 1930.

A new spatially and temporally variable sigma parameter in degree-day melt

A. E. Jowett et al.

Title Page

Abstract

Introduction

Conclusions

References

Tables

Figures

◀

▶

◀

▶

Back

Close

Full Screen / Esc

Printer-friendly Version

Interactive Discussion



Summer is the dominant season in the melt calculation as this is when most melting takes place. Moreover, the higher σ values above the ELA are generally of little consequence as these are in line with the constant σ values previously used. It is therefore values below the ELA during the melt season that will have most effect on the melt calculation. As the summer (especially July) σ values are consistently lower than 4.2°C , this has implications for the modelled melt and therefore SMB of the GrIS for the study period. As previously discussed, lower constant σ values yield a decreased modelled melt area and a higher SMB (Fausto et al., 2009a). However, the variable parameter will likely affect the total melt volume rather than melt area as lower σ values are evident largely below the ELA during the melt season. Our results give a mean 1870–2013 summer σ value averaged across the entire ice sheet of $\sim 3.2^\circ\text{C}$, which is $\sim 1\text{--}2^\circ\text{C}$ lower than in many studies. Indeed some values around the ice sheet periphery are at least five times smaller than some constant parameters discussed in Rogozhina and Rau (2014). Our summer σ values range from $0\text{--}5^\circ\text{C}$ over the whole ice sheet and $0\text{--}4^\circ\text{C}$ in the ablation zone. These values are overall higher than the $1\text{--}2.5^\circ\text{C}$ that Rogozhina and Rau (2014) obtained for summer σ based on ERA-40 reanalysis from 1958–2001. Their shorter time series, different model used and lower spatial resolution ($10\text{km} \times 10\text{km}$ compared to our $5\text{km} \times 5\text{km}$), which tends to smear the edges of the ice sheet, are likely to account for some of the differences in calculated σ .

The statistically significant increases in σ through time over the study period in Fig. 11 would predict that the melt area has increased on average for the last 144 years. This would result in a downward trend in SMB from 1870–2013, in line with the results of Rogozhina and Rau (2014) to be investigated in a planned study into SMB of the GrIS using our variable σ . Part of this trend may, however, be due to an increasing number of weather stations assimilated into the 20CR series capturing more surface air temperature variability during the second half of the reanalysis period.

There is considerable variation in the spatial distribution of σ on both the inter- and intra-annual timescales for the period of study. Banding with elevation is evident in all seasons, in agreement with the findings of Fausto et al. (2009b), but is less evi-

A new spatially and temporally variable sigma parameter in degree-day melt

A. E. Jowett et al.

Title Page

Abstract

Introduction

Conclusions

References

Tables

Figures

◀

▶

◀

▶

Back

Close

Full Screen / Esc

Printer-friendly Version

Interactive Discussion



dent in the summer months. Higher σ values in the centre of the ice sheet in Fig. 6 can be attributed to the effects of continentality and dominant more stable weather patterns with predominantly clearer skies further inland (Taurisano et al., 2004). The lower σ values in coastal areas may be attributed to temperature inversions and greater cloud cover (suppressing the diurnal temperature range) for much of the year (Cappelen et al., 2001; Mernild and Liston, 2010). The south-west of the GrIS also tends to have higher σ values due to transient low-pressure systems moving eastwards from the Labrador Sea, especially in summer. Winter σ values tend to be larger (Fig. 6) due to the intense cold that often dominates the centre of the ice sheet during these months, which is sometimes interrupted by the intrusion of transient weather systems, especially in the south and south east, thus leading to large shifts in temperature (Box, 2002; Hanna et al., 2012). The banding with elevation is less noticeable during the summer months due to the limiting effect of melt on near-surface temperatures, as discussed previously.

The spatial and temporal variations in σ across the GrIS underscore the importance of including a variable parameter in the temperature-index method. As Fausto et al. (2009a) found a 33% difference in melt area with a $\sim 2^\circ\text{C}$ variation in a spatially and temporally constant σ , following their results the $\sim 1^\circ\text{C}$ lower summer σ found here could reduce the melt area by over 15%. The impact of this change in melt area on the SMB, particularly during summer months: will be quantified using our updated version of the Janssens and Huybrechts (2000) PDD model. The effect of increased σ in other months and seasons also needs to be investigated to determine whether this compensates in part for the effect of lower summer σ or has little impact on the melt calculation. This will be presented elsewhere.

Validation of the new σ parameter is difficult due to the limited spatial and temporal coverage of in situ surface air temperature observational data available for Greenland. There is inevitably more data available for areas around and surrounding the ice-sheet margin, which may introduce bias into the validation, alongside some issues concerning the independence of the validation and reanalysis meteorological datasets. As the

A new spatially and temporally variable sigma parameter in degree-day melt

A. E. Jowett et al.

Title Page

Abstract

Introduction

Conclusions

References

Tables

Figures

◀

▶

◀

▶

Back

Close

Full Screen / Esc

Printer-friendly Version

Interactive Discussion



Figure 13 shows high correlation coefficients of 0.73, 0.76, 0.79 and 0.82 for annual, spring, autumn and winter respectively. These correlation coefficients are all statistically significant showing a strong positive significant relationship between temperature variability calculated from 20CR and ERA-I for the overlap period 1979–2008. The summer and July plots however, show weaker correlations between 20CR and ERA-I, with a positive bias in 20CR compared to ERA-I of $\sim 0.76^{\circ}\text{C}$ in summer and 0.7°C in July for the overlap period. These correlations are still statistically significant, showing there is a significant relationship between 20CR and ERA-I σ from 1979–2008, despite the spread about the trend line.

A unique aspect of the present work is the assessment of trends in σ over the last 144 years for each $5\text{ km} \times 5\text{ km}$ pixel on the ice sheet. The significant trends in σ across the ice sheet shown in all plots (with the two previously-highlighted exceptions) indicate that σ has increased from 1870–2013 and therefore temperatures have become more variable across the ice sheet over the last 144 years. This increase is especially prominent in the southern region for all plots, and also in the north-west for all seasons. Other studies (e.g. Hall et al., 2013) have found the greatest increase in temperatures in these regions of the GrIS, indicating that not only are these regions becoming warmer, but they have also experienced increased high-frequency (sub-monthly) temperature variability. This is unsurprising given the extent of recent warming with accompanying more frequent and extreme warm air/melt episodes over Greenland (Hanna et al., 2008, 2014; Overland et al., 2012, 2015), and stronger Greenland high-pressure blocking coupled with increasingly variable winter NAO over the last 100 years (Hanna et al., 2013, 2015). Also the assimilation of more weather stations into 20CR during the latter half of the 1870–2013 period is likely to have had an adverse effect of increasing variability in temperatures because this enhances the effective spatial resolution and sensitivity of the reanalysis. On the other hand, given the positive bias in 20CR σ shown in Fig. 13, the 1870–2013 trend may be an underestimate if ERA-I is assumed to be the more accurate re-analysis and therefore 20CR is overestimating variability. The balance of these various effects will influence the observed trend.

A new spatially and temporally variable sigma parameter in degree-day melt

A. E. Jowett et al.

Title Page

Abstract

Introduction

Conclusions

References

Tables

Figures

◀

▶

◀

▶

Back

Close

Full Screen / Esc

Printer-friendly Version

Interactive Discussion



However, when the more recent period (1990–2013) is examined separately, the trends become more complex with fewer areas of statistical significance than for the 144 year trend. The presence of negative trends in all these plots for the shorter/recent timescale suggests that temperatures became less variable across large parts of the ice sheet during this period. Interestingly, in the north-west in July there is a statistically significant area of reduced σ , indicating reduced temperature variability here since 1990. This could be due to more widespread, intense and longer-lasting summer melt suppressing near-surface air temperatures at around freezing for longer in summer. This was coincident with a time of more negative summer NAO, leading to more southerly warm air advection and amplified Greenland warming in the last 1–2 decades (Hanna et al., 2015; Overland et al., 2012, 2014).

Figure 14 shows correlations between σ and NAOI/GBI for summer for different time periods. The GBI-v.- σ plot for 1990–2013 shows significant negative correlations (< -0.4) along parts of the western margin, going slightly inland, and in extreme north-west Greenland. Temperature variability is less in these regions with high GBI, due to more stable prevailing weather conditions under high pressure. There is an opposite, negative correlation along the southeast Greenland coast due to this being on the other side of the high pressure block and therefore more subject to associated vagaries in weather conditions, e.g. sometimes affected by strong cold northerly winds flowing south along the Denmark Strait due to changes in the position/intensity of the High. The pattern of GBI- σ correlations for 1948–2013 is similar but somewhat muted (but is broadly similar as significance levels are then lower). The NAO-v.- σ 1899–2013 plot shows modest but significant positive correlations over most of the GrIS, which are associated with less blocking and more variable temperatures under a high NAO regime. The NAO- σ plot for 1990–2013 shows an area of significant negative correlation in inland southeast Greenland, which rather resembles the area of opposite correlation in the GBI- σ plot for the same time period.

5 Conclusions

This work uniquely builds on previous studies by extending the timescale of currently available monthly σ grids back to 1870 by using post-processed 20CR surface air temperature dataset as input to the standard deviation. This goes some way towards answering the call for “realistic σ values under climate conditions different from today” by Seguinot and Rogozhina (2014). To our knowledge, no other studies have determined σ from ERA-I at the 5 km scale, nor have they utilised 20CR to compute σ fields. Although the 20CR series may be considered less accurate than other products (e.g. ERA-I), the inclusion of our new three-step correction procedure helps mitigate against the inaccuracies of the series, as evidenced by the promising validation results. The use of the resulting spliced 144 year temperature/ σ annual/seasonal/monthly time series has enabled a more thorough investigation into trends of temperature variability across the GrIS on a variety of timescales than has previously been possible. Our new σ parameter shows large deviations from the commonly assumed value of 4.2 °C, particularly during the summer months when melt intensifies. We therefore conclude that incorporating our spatially and temporally varying σ factor provides a marked improvement over using a constant σ value, especially for the early part of the record where σ is shown to be much lower than many values prescribed in the literature for summer. Moreover, given the high temporal and spatial variability of σ , our results suggest that it is best to calculate σ values each month, for example in x -hourly timesteps, before application of any PDD model. Also we argue that a constant σ value cannot be used for future projections as the predicted increase in summer temperatures should result in a reduced σ as the surface temperature is limited to 0 °C.

This work offers a more comprehensive validation of ERA-I/20CR based σ against AWS data than previous studies, as here we have incorporated 67 sites from across the ice sheet. The overall agreement between modelled and observed σ indicates that our new parameter realistically approximates sub-monthly temperature variability at the 5 km scale across the GrIS. Our trends show a clear increase in σ across the ice sheet

TCD

9, 5327–5371, 2015

A new spatially and temporally variable sigma parameter in degree-day melt

A. E. Jowett et al.

Title Page

Abstract

Introduction

Conclusions

References

Tables

Figures

◀

▶

◀

▶

Back

Close

Full Screen / Esc

Printer-friendly Version

Interactive Discussion



A new spatially and temporally variable sigma parameter in degree-day melt

A. E. Jowett et al.

Title Page

Abstract

Introduction

Conclusions

References

Tables

Figures

◀

▶

◀

▶

Back

Close

Full Screen / Esc

Printer-friendly Version

Interactive Discussion



from 1870–2013, which adds to the recent weight of evidence for increasing climatic variability over the ice sheet. Over the recent short period 1990–2013, the temporal trends expressed by σ illustrate how regionally variable this parameter is, despite the lack of statistical significance in most areas. Based on the preceding analysis, we conclude that our results provide a more realistic long-term (1870–2013) parameter of σ for input into PDD models of the GrIS SMB.

Acknowledgements. We would like to thank the Natural Environment Research Council for funding this PhD (NERC reference number NE/K500914/1). Further acknowledgement must be extended to the Danish Meteorological Institute, the Greenland Climate Network, Programme for Monitoring of the Greenland Ice Sheet, the National Centre for Atmospheric Research, Computational and Information Systems Laboratory for providing 20CR version 2 data and the European Centre for Medium-Range Weather Forecasts for providing data without which this work would not have been possible. Within the department of Geography at the University of Sheffield we would like to thank David McCutcheon for his cartography skills in re-drafting our figures.

References

- Ahlstrøm, A. P. and PROMICE team: A new programme for monitoring the mass loss of the Greenland ice sheet, *Geol. Surv. Den. Greenl.*, 15, 61–64, 2008.
- Box, J. E.: Survey of Greenland instrumental temperature records: 1873–2001, *Int. J. Climatol.*, 22, 1829–1847, 2002.
- Braithwaite, R. J.: Calculation of degree-days for glacier-climate research, *Z. Gletscherk. Glazialgeol.*, 20, 1–8, 1984.
- Braithwaite, R. J.: Positive degree-day factors for ablation on the Greenland ice sheet studied by energy-balance modelling, *J. Glaciol.*, 41, 153–160, 1995.
- Cappelen, J., Jørgensen, B. V., Laursen, E. V., and Thomsen, L.: The observed climate of Greenland, 1958–99 – with climatological standard normal, 1961–90, DMI Technical Report 00-18, DMI, Copenhagen, 2001.

A new spatially and temporally variable sigma parameter in degree-day melt

A. E. Jowett et al.

Title Page

Abstract

Introduction

Conclusions

References

Tables

Figures



Back

Close

Full Screen / Esc

Printer-friendly Version

Interactive Discussion

Cappelen, J., Laursen, E. V., Kern-Hansen, K., Boas, L., Wang, P. R., Jørgensen, B. V., and Carstensen, L. S.: Weather observations from Greenland 1958–2012, DMI Technical Report 13-11, DMI, Copenhagen, 2013.

Compo, G. P., Whitaker, J. S., and Sardeshmukh, P. D.: Feasibility of a 100 year reanalysis using only surface pressure data, *B. Am. Meteorol. Soc.*, 87, 175–190, 2006.

Compo, G. P., Whitaker, J. S., Sardeshmukh, P. D., Matsui, N., Allan, R. J., Yin, X., Gleason, B. E., Vose, R. S., Rutledge, G., Bessemoulin, P., Brönnimann, S., Brunet, M., Crouthamel, R. I., Grant, A. N., Groisman, P. Y., Jones, P. D., Kruk, M. C., Kruger, A. C., Marshall, G. J., Maugeri, M., Mok, H. Y., Nordli, Ø., Ross, T. F., Trigo, R. M., Wang, X. L., Woodruff, S. D., and Worley, S. J.: The Twentieth Century Reanalysis Project, *Q. J. Roy. Meteorol. Soc.*, 137, 1–28, doi:10.1002/qj.776, 2011.

Danish Meteorological Institute: Quality control of Greenlandic weather and climate data series 1958–2010: Supplement to Technical Report 11-15, DMI Ministry of Climate and Energy, Copenhagen, 2011.

Dee, D. P., Uppala, S. M., Simmons, A. J., Berrisford, P., Poli, P., Kobayashi, S., Andrae, U., Balmaseda, M. A., Balsamo, G., Bauer, P., Bechtold, P., Beljaars, A. C. M., van de Berg, L., Bidlot, J., Bormann, N., Delsol, C., Dragani, R., Fuentes, M., Geer, A. J., Haimberger, L., Healy, S. B., Hersbach, H., Hólm, E. V., Isaksen, L., Kållberg, P., Köhler, M., Matricardi, M., McNally, A. P., Monge-Sanz, B. M., Morcrette, J.-J., Park, B.-K., Peubey, C., de Rosnay, P., Tavolato, C., Thépaut, J.-N. and Vitart, F.: The ERA-Interim reanalysis: configuration and performance of the data assimilation system, *Q. J. Roy. Meteorol. Soc.*, 137, 553–597, doi:10.1002/qj.828, 2011.

Ekholm, S.: A full coverage, high-resolution, topographic model of Greenland computed from a variety of digital elevation data, *J. Geophys. Res.*, 101, 21961–21972, 1996.

Fausto, R. S., Ahlstrøm, A. P., Van As, D., Bøggild, C. E., and Johnsen, S. J.: A new present-day temperature parameterization for Greenland, *J. Glaciol.*, 55, 95–105, 2009a.

Fausto, R. S., Ahlstrøm, A. P., Van As, D., Johnsen, S. J., Langen, P. L., and Steffen, K.: Improving surface boundary conditions with focus on coupling snow densification and meltwater retention in large-scale ice-sheet models of Greenland, *J. Glaciol.*, 55, 869–878, 2009b.

Fausto, R. S., Ahlstrøm, A. P., Van As, D., and Steffen, K.: Present-day temperature standard deviation parameterization for Greenland, *J. Climate*, 57, 1181–1183, 2011.

A new spatially and temporally variable sigma parameter in degree-day melt

A. E. Jowett et al.

[Title Page](#)[Abstract](#)[Introduction](#)[Conclusions](#)[References](#)[Tables](#)[Figures](#)[◀](#)[▶](#)[◀](#)[▶](#)[Back](#)[Close](#)[Full Screen / Esc](#)[Printer-friendly Version](#)[Interactive Discussion](#)

Ferguson, C. R. and Villarini, G.: Detecting inhomogeneities in the Twentieth Century Reanalysis over the central United States, *J. Geophys. Res.*, 117, D05123, doi:10.1029/2011JD016988, 2012.

Ferguson, C. R. and Villarini, G.: An evaluation of the statistical homogeneity of the Twentieth Century Reanalysis, *Clim. Dynam.*, 42, 2841–2866, 2014.

Hall, D. K., Comiso, J. C., DiGirolamo, N. E., Shuman, C. A., Box, J. E., and Koenig, L. S.: Variability in surface temperature and melt extent of the Greenland ice sheet from MODIS, *Geophys. Res. Lett.*, 40, 2114–2120, 2013.

Hanna, E. and Valdes, P.: Validation of ECMWF (re)analysis surface climate data, 1979–1998, for Greenland and implications for mass balance modelling of the ice sheet, *Int. J. Climatol.*, 21, 171–195, 2001.

Hanna, E., Huybrechts, P., Janssens, I., Cappelen, J., Steffen, K., and Stephens, A.: Runoff and mass balance of the Greenland ice sheet: 1958–2003, *J. Geophys. Res.*, 110, D13108, doi:10.1029/2004JD005641, 2005.

Hanna, E., Huybrechts, P., Steffen, K., Cappelen, J., Huff, R., Shuman, C., Irvine-Fynn, T., Wise, S., and Griffiths, M.: Increased runoff from melt from the Greenland Ice Sheet: a response to global warming, *J. Climate*, 21, 331–341, 2008.

Hanna, E., Huybrechts, P., Cappelen, J., Steffen, K., Bales, R. C., Burgess, E., McConnell, J. R., Steffensen, J. P., Van den Brooke, M., Wake, L., Bigg, G., Griffiths, M., and Savas, D.: Greenland Ice Sheet surface mass balance 1870 to 2010 based on Twentieth Century Reanalysis, and links with global climate forcing, *J. Geophys. Res.*, 116, D24121, doi:10.1029/2011JD016387, 2011.

Hanna, E., Mernild, S. H., Cappelen, J., and Steffen, K.: Recent warming in Greenland in a long-term instrumental (1881–2012) climatic context: 1. Evaluation of surface air temperature records, *Environ. Res. Lett.*, 7, 045404, doi:10.1088/1748-9326/7/4/045404, 2012.

Hanna, E., Jones, J. M., Cappelen, J., Mernild, S. H., Wood, L., Steffen, K., and Huybrechts, P.: The influence of North Atlantic atmospheric and oceanic forcing effects on 1900–2010 Greenland summer climate and ice melt/runoff, *Int. J. Climatol.*, 33, 862–880, 2013.

Hanna, E., Fettweis, X., Mernild, S. H., Cappelen, J., Ribergaard, M. H., Shuman, C. A., Steffen, K., Wood, L., and Mote, T. L.: Atmospheric and oceanic climate forcing of the exceptional Greenland ice sheet surface melt in summer 2012, *Int. J. Climatol.*, 34, 1022–1037, 2014.

Hanna, E., Cropper, T. E., Jones, P. D., Scaife, A. A., and Allan, R.: Recent seasonal asymmetric changes in the NAO (a marked summer decline and increased winter variability) and asso-

A new spatially and temporally variable sigma parameter in degree-day melt

A. E. Jowett et al.

Title Page

Abstract

Introduction

Conclusions

References

Tables

Figures



Back

Close

Full Screen / Esc

Printer-friendly Version

Interactive Discussion

ciated changes in the AO and Greenland Blocking Index, *Int. J. Climatol.*, 35, 2540–2554, doi:10.1002/joc.4157, 2015.

Hock, R.: Temperature index melt modelling in mountain areas, *J. Hydrol.*, 282, 104–115, 2003.

Huybrechts, P. and de Wolde, J.: The dynamic response of the Greenland and Antarctic ice sheets to multiple-century climatic warming, *J. Climate*, 12, 2169–2188, 1999.

Janssens, I. and Huybrechts, P.: The treatment of meltwater retention in mass balance parameterizations of the Greenland ice sheet, *Ann. Glaciol.*, 31, 133–140, 2000.

Lefebre, F., Gallée, H., Van Ypersele, J.-P., and Huybrechts, P.: Modelling of large-scale melt parameters with a regional climate model in south Greenland during the 1991 melt season, *Ann. Glaciol.*, 32, 391–397, 2002.

Mernild, S. H. and Liston, G. E.: The influence of air temperature inversions on snowmelt and glacier mass balance simulations, Ammassalik Island, Southeast Greenland, *J. Appl. Meteorol. Clim.*, 49, 47–67, 2010.

Overland, J. E., Francis, J. A., Hanna, E., and Wang, M.: The recent shift in early summer Arctic atmospheric circulation, *Geophys. Res. Lett.*, 39, L19804, doi:10.1029/2012GL053268, 2012.

Overland, J. E., Hanna, E., Hanssen-Bauer, I., Kim, S.-J., Walsh, J., Wang, M., and Bhatt, U. S.: Air temperature [in Arctic Report Card 2014], available at: www.arctic.noaa.gov/reportcard (last access: 27 August 2015), 2014.

Overland, J. E., Francis, J., Hall, R. J., Hanna, E., Kim, S.-J., and Vihma, T.: The melting Arctic and mid-latitude weather patterns: are they connected?, *J. Climate*, doi:10.1175/JCLI-D-14-00822.1, in press, 2015.

Radić, V. and Hock, R.: Modeling future glacier mass balance and volume changes using ERA-40 reanalysis and climate models: a sensitivity study at Storglaciären, Sweden, *J. Geophys. Res.*, 111, F03003, doi:10.1029/2005JF000440, 2006.

Reeh, N.: Parameterization of melt rate and surface temperature on the Greenland ice sheet, *Polarforschung*, 59, 113–128, 1991.

Ritz, C., Kanagaratnam, P., and Letréguilly, A.: Sensitivity of a Greenland ice sheet model to ice flow and ablation parameters: consequences for the evolution through the last glacial cycle, *Clim. Dynam.*, 13, 11–24, 1997.

Rogozhina, I. and Rau, D.: Vital role of daily temperature variability in surface mass balance parameterizations of the Greenland Ice Sheet, *The Cryosphere*, 8, 575–585, doi:10.5194/tc-8-575-2014, 2014.

A new spatially and temporally variable sigma parameter in degree-day melt

A. E. Jowett et al.

Title Page

Abstract

Introduction

Conclusions

References

Tables

Figures



Back

Close

Full Screen / Esc

Printer-friendly Version

Interactive Discussion



- Seguinot, J.: Spatial and seasonal effects of temperature variability in a positive degree-day glacier surface mass-balance model, *J. Glaciol.*, 59, 1202–1204, 2013.
- Seguinot, J. and Rogozhina, I.: Daily temperature variability predetermined by thermal conditions over ice-sheet surfaces, *J. Glaciol.*, 60, 603–605, 2014.
- 5 Steffen, K. and Box, J. E.: Surface climatology of the Greenland ice sheet: Greenland Climate Network 1995–1999, *J. Geophys. Res.*, 106, 33951–33964, 2001.
- Steffen, K., Box, J. E., and Abdalati, W.: Greenland Climate Network: CG-Net in Colbeck, S. C., CRREL 96-27 Special Report on Glaciers, Ice Sheets and Volcanoes, trib. to M. Meier, US Army Corp of Engineers Cold Regions Research and Engineering Laboratory, Hanover, NH, 98–103, 1996.
- 10 Taurisano, A., Bøggild, C. E., and Karlsen, H. G.: A century of climate variability and climate gradients from coast to ice sheet in West Greenland, *Geograf. Ann. A*, 86, 217–224, 2004.
- Uppala, S. M., Kållberg, P. W., Simmons, A. J., Andrae, U., Bechtold, V. D. C., Fiorino, M., Gibson, J. K., Haseler, J., Hernandez, A., Kelly, G. A., Li, X., Onogi, K., Saarinen, S., Sokka, N., Allan, R. P., Andersson, E., Arpe, K., Balmaseda, M. A., Beljaars, A. C. M., Berg, L. V. D., Bidlot, J., Bormann, N., Caires, S., Chevallier, F., Dethof, A., Dragosavac, M., Fisher, M., Fuentes, M., Hagemann, S., Hólm, E., Hoskins, B. J., Isaksen, L., Janssen, P. A. E. M., Jenne, R., McNally, A. P., Mahfouf, J.-F., Morcrette, J.-J., Rayner, N. A., Saunders, R. W., Simon, P., Sterl, A., Trenberth, K. E., Untch, A., Vasiljevic, D., Viterbo, P., and Woollen, J.: The ERA-40 re-analysis, *Q. J. Roy. Meteorol. Soc.*, 131, 2961–3012, doi:10.1256/qj.04.176, 2005.
- 20 van As, D., Fausto, R. S., and the PROMICE project team: Programme for monitoring of the Greenland Ice Sheet (PROMICE): first temperature and ablation records, *Geol. Surv. Den. Greenl.*, 23, 73–76, 2011.
- 25 Van de Wal, R. S. W., Boot, W., van den Brooke, M. R., Smeets, C. J. P. P., Reijmer, C. H., Donker, J. J. A., and Oerlemans, J.: Large and rapid melt-induced velocity changes in the ablation zone of the Greenland Ice Sheet, *Science*, 321, 111–113, 2008.
- Wake, L. M. and Marshall, S. J.: Assessment of current methods of positive degree-day calculation using in situ observations from glaciated regions, *J. Glaciol.*, 61, 329–344, 2015.
- 30 Wake, L. M., Huybrechts, P., Box, J. E., Hanna, E., Janssens, I., and Milne, G. A.: Surface mass-balance changes of the Greenland ice sheet since 1866, *Ann. Glaciol.*, 50, 178–184, 2009.

A new spatially and temporally variable sigma parameter in degree-day melt

A. E. Jowett et al.

Table 1. The five months where breakpoints were detected are displayed at the top of the table. The year at which the breakpoint for that month was detected is displayed below, followed by the confidence intervals in 2 m air temperature from 1870–2013. These were identified using Bai–Perron breakpoint analysis in R . The results displayed here are those for the months where breakpoints were identified in both the 2 m air temperature and the spread of 2 m air temperature, deemed to be due to the model, not climatology. The mean 2 m air temperature before and after the breakpoint for each month is also displayed along with the difference between them. This difference (displayed to 2 d.p. here) was taken as the correction factor and applied to 3 hourly and monthly 2 m air temperature before the breakpoint for that month.

Month of breakpoint	Mar	Apr	Aug	Sep	Oct
Year of breakpoint	1946	1941	1912	1941	1966
Confidence Intervals	1930–1959	1921–1948	1872–1927	1899–1966	1941–1985
Mean before breakpoint (°C)	–27.79	–21.85	–7.89	–14.69	–21.68
Mean after breakpoint (°C)	–29.87	–23.45	–8.61	–15.64	–23.12
Difference (°C)	2.08	1.6	0.72	0.95	1.44

Title Page

Abstract

Introduction

Conclusions

References

Tables

Figures

◀

▶

◀

▶

Back

Close

Full Screen / Esc

Printer-friendly Version

Interactive Discussion



A new spatially and temporally variable sigma parameter in degree-day melt

A. E. Jowett et al.

Title Page

Abstract

Introduction

Conclusions

References

Tables

Figures

◀

▶

◀

▶

Back

Close

Full Screen / Esc

Printer-friendly Version

Interactive Discussion



Table 3. Annual, summer and July modelled σ and that derived from GC-Net AWS observations for the period since the mid-1990s.

Station name	Altitude (m)	Period	σ_a	σ_a^m	Diff.	σ_{jja}	σ_{jja}^m	Diff.	σ_j	σ_j^m	Diff.
Peterman Gl.	37	2002–2006	5.28	4.98	-0.31	3.61	2.29	-1.32	3.38	1.72	-1.66
JAR3	283	2000–2004	4.66	5.39	0.73	1.95	3.27	1.32	1.56	3.09	1.53
JAR 2	507	1999–2012	4.70	5.28	0.59	1.68	3.18	1.50	1.38	3.05	1.68
JAR 1	932	1997–2012	4.92	5.33	0.41	2.15	3.02	0.87	1.91	2.90	0.98
Peterman ELA	965	2003–2012	–	–	–	2.88	2.60	-0.28	1.26	1.53	0.26
Swiss Camp	1176	1996–2012	5.50	5.38	-0.11	2.65	3.01	0.36	2.13	2.85	0.71
GITS	1869	1995–2007	5.78	4.90	-0.88	3.50	2.93	-0.57	3.15	2.41	-0.74
Crawford P2	1990	1997–2001	6.82	5.53	-1.29	4.18	3.18	-1.00	3.80	2.94	-0.86
Humboldt	1995	1995–2012	6.32	5.22	-1.10	4.11	3.11	-1.00	3.37	2.52	-0.84
Crawford Pt. 1	2022	1995–2012	6.75	5.58	-1.17	4.19	3.13	-1.06	3.88	2.89	-0.99
Tunu-N	2052	1996–2012	5.86	5.03	-0.82	4.28	3.27	-1.00	3.39	2.52	-0.87
DYE-2	2099	1996–2012	6.82	5.64	-1.18	4.27	3.42	-0.85	3.79	3.18	-0.61
NASA-U	2334	1995–2012	6.95	5.64	-1.31	4.34	3.26	-1.07	4.07	2.93	-1.14
NASA-SE	2373	1998–2012	6.89	5.33	-1.56	4.67	3.45	-1.22	4.33	3.28	-1.05
NEEM	2454	2006–2012	6.45	5.56	-0.89	4.39	3.08	-1.31	3.78	2.62	-1.16
Saddle	2467	1997–2012	6.58	5.63	-0.95	4.42	3.56	-0.86	3.96	3.39	-0.57
KAR	2579	1999–2001	6.32	4.85	-1.47	5.02	3.71	-1.31	4.61	3.39	-1.22
NASA-E	2614	1997–2011	6.05	5.12	-0.93	4.53	3.51	-1.01	3.63	2.71	-0.92
South Dome	2901	2003–2012	6.04	5.36	-0.68	4.09	3.69	-0.40	4.04	3.81	-0.23
NGRIP	2941	2002–2010	6.93	5.92	-1.01	4.65	3.48	-1.17	4.07	3.26	-0.81
Summit	3199	1996–2012	6.80	5.99	-0.81	5.13	3.94	-1.19	4.40	3.36	-1.04

A new spatially and temporally variable sigma parameter in degree-day melt

A. E. Jowett et al.

Title Page

Abstract

Introduction

Conclusions

References

Tables

Figures

◀

▶

◀

▶

Back

Close

Full Screen / Esc

Printer-friendly Version

Interactive Discussion



Table 4. Annual, summer and July modelled σ and that derived from PROMICE AWS observations since 2007, with data spanning the ablation and accumulation zones of the ice sheet.

Station	Altitude (m)	Period	σ_a	σ_a^m	Diff.	σ_{jja}	σ_{jja}^m	Diff.	σ_j	σ_j^m	Diff.
UPE_L	230	2009–2012	4.24	4.77	0.54	1.88	2.60	0.72	1.47	2.14	0.67
TAS_L	270	2007–2012	2.86	3.86	1.00	1.68	2.33	0.65	1.37	2.10	0.73
QAS_L	310	2007–2012	3.80	3.83	0.03	1.57	2.23	0.66	1.54	2.10	0.56
KAN_B	350	2011–2012	5.48	6.27	0.80	2.41	3.37	0.96	1.99	3.10	1.11
KPC_L	380	2008–2012	3.86	3.82	−0.04	2.52	2.46	−0.07	2.01	2.14	0.13
MIT	460	2009–2012	3.53	3.67	0.14	1.94	2.33	0.39	1.84	2.01	0.17
SCO_L	470	2008–2012	3.93	4.53	0.60	1.71	3.34	1.63	1.47	2.74	1.27
NUK_L	560	2008–2012	5.04	5.98	0.94	1.93	3.10	1.18	1.81	3.08	1.27
THU_L	570	2010–2012	3.98	4.05	0.07	2.21	1.81	−0.40	1.64	1.45	−0.19
TAS_U	580	2008–2012	3.46	3.96	0.50	1.50	2.33	0.83	1.25	2.13	0.88
KAN_L	680	2009–2012	4.98	5.65	0.67	1.61	3.22	1.61	1.53	3.27	1.73
THU_U	770	2010–2012	4.37	4.11	−0.26	2.29	1.83	−0.46	1.72	1.47	−0.26
KPC_U	870	2009–2012	4.74	4.21	−0.53	2.70	2.63	−0.07	1.72	2.05	0.33
QAS_U	890	2008–2012	3.60	4.26	0.66	1.92	2.37	0.45	1.42	2.29	0.87
NUK_N	930	2010–2012				1.65	2.92	1.27	1.12	2.64	1.52
UPE_U	980	2009–2012	4.86	5.49	0.62	1.83	3.03	1.20	1.28	2.45	1.17
SCO_U	1000	2008–2012	4.21	4.50	0.29	2.16	3.43	1.27	1.51	2.79	1.27
NUK_U	1140	2007–2012	5.07	5.86	0.79	1.88	3.10	1.22	1.49	2.73	1.24
KAN_M	1270	2009–2012	5.67	5.61	−0.06	2.14	3.03	0.88	1.77	3.07	1.29
KAN_U	1850	2009–2012				3.56	3.44	−0.11	3.09	3.51	0.42
UPE_L	230	2009–2012	4.24	4.77	0.54	1.88	2.60	0.72	1.47	2.14	0.67
TAS_L	270	2007–2012	2.86	3.86	1.00	1.68	2.33	0.65	1.37	2.10	0.73

A new spatially and temporally variable sigma parameter in degree-day melt

A. E. Jowett et al.

Title Page

Abstract

Introduction

Conclusions

References

Tables

Figures



Back

Close

Full Screen / Esc

Printer-friendly Version

Interactive Discussion

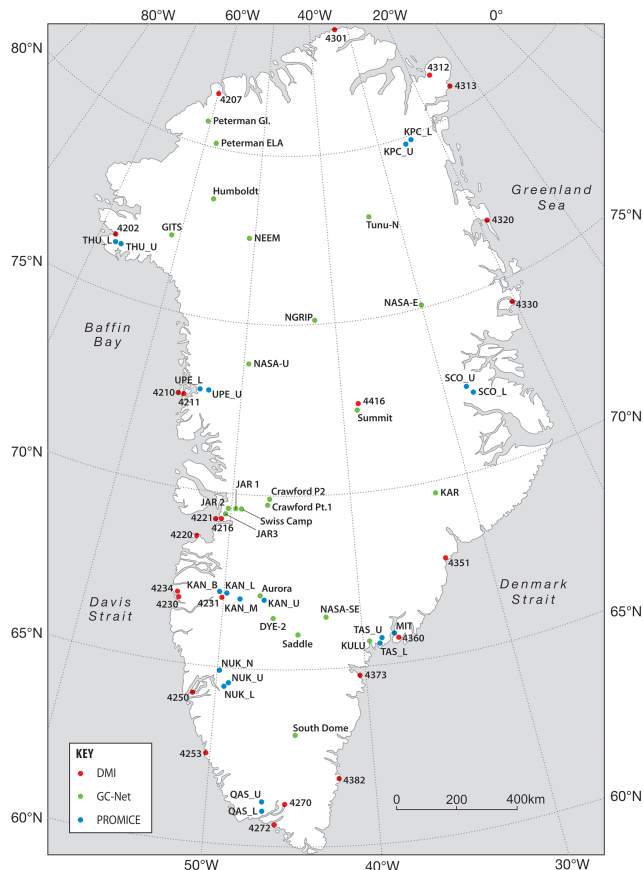


Figure 1. Location map of the DMI, GC-Net and PROMICE AWS providing the observed 2 m air temperature data used in the validation of our new variable σ parameter.

A new spatially and temporally variable sigma parameter in degree-day melt

A. E. Jowett et al.

Title Page

Abstract

Introduction

Conclusions

References

Tables

Figures



Back

Close

Full Screen / Esc

Printer-friendly Version

Interactive Discussion

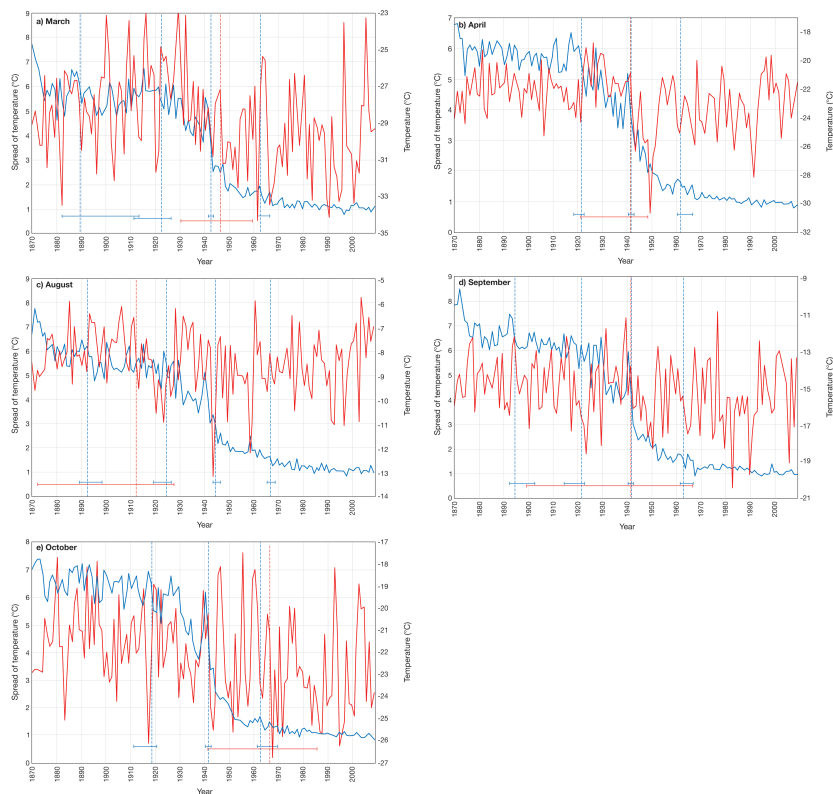


Figure 2. (a) March, (b), April, (c) August, (d) September, and (e) October breakpoints (vertical lines) in ice sheet averaged 2 m air temperature (red) and the spread of 2 m air temperatures (blue) from 1870–2013, with confidence intervals (horizontal lines) determined from Bai–Perron breakpoint analysis in R. The mean 2 m air temperatures before and after each breakpoint and the correction factors for those months where the confidence intervals overlap are shown in Table 1.

A new spatially and temporally variable sigma parameter in degree-day melt

A. E. Jowett et al.

Title Page

Abstract

Introduction

Conclusions

References

Tables

Figures



Back

Close

Full Screen / Esc

Printer-friendly Version

Interactive Discussion

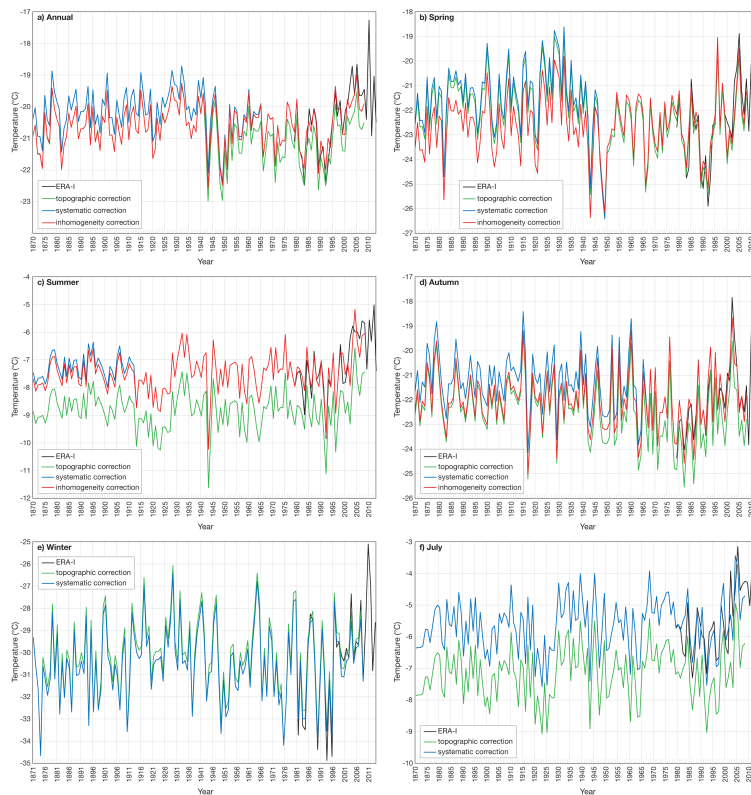


Figure 3. (a) Annual, (b) spring, (c) summer, (d) autumn, (e) winter and (f) July ice sheet averaged GrIS 2 m air temperature from 1870–2013 inclusive calculated from 6 hourly downscaled, corrected ERA-I (black line) and from 3 hourly 20CR corrected for the effect of orography (topographic correction; green line), systematic correction factor applied to scale 20CR to ERA-I (blue line) and including the correction(s) for artificial breaks (inhomogeneity correction; red line). Note the different y axis ranges.

A new spatially and temporally variable sigma parameter in degree-day melt

A. E. Jowett et al.

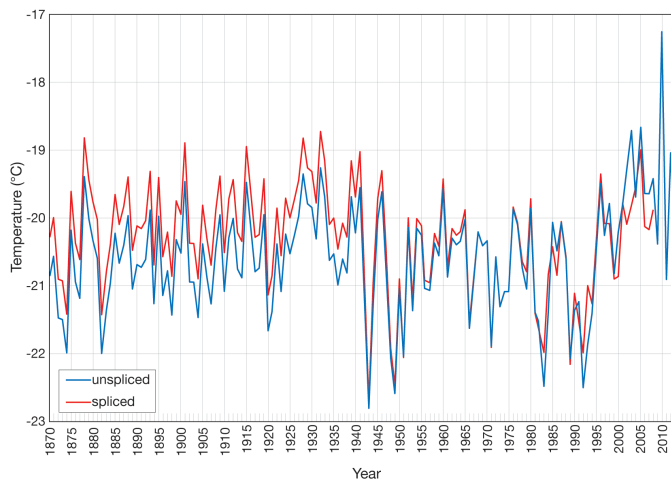


Figure 4. Ice sheet average annual *spliced* temperature series (blue line) calculated from 20CR (1870–1978) incorporating scaling to ERA-I and breakpoint correction factors and ERA-I (1979–2013), compared to the *unspliced* 20CR downscaled, corrected for the effect of orography and scaled to ERA-I (red line), highlighting the differences between 20CR and ERA-I for the overlap period.

[Title Page](#)[Abstract](#)[Introduction](#)[Conclusions](#)[References](#)[Tables](#)[Figures](#)[Back](#)[Close](#)[Full Screen / Esc](#)[Printer-friendly Version](#)[Interactive Discussion](#)

A new spatially and temporally variable sigma parameter in degree-day melt

A. E. Jowett et al.

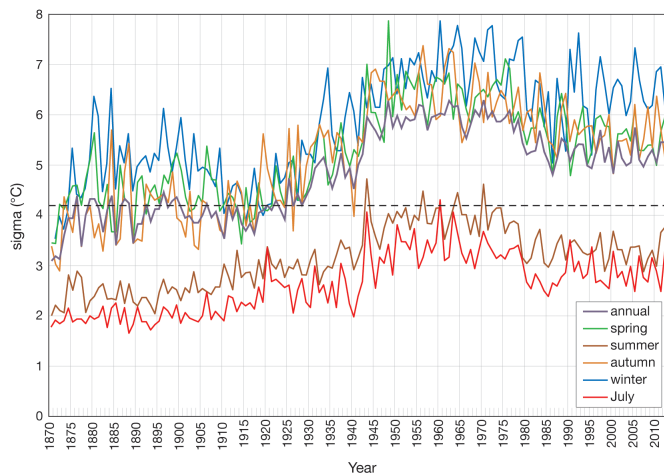


Figure 5. Annual, seasonal and July ice sheet average σ from 1870–2013 calculated from spliced, fully corrected 20CR (1870–1978) and ERA-I (1979–2013) 2 m air temperatures, illustrating inter-annual fluctuations in σ . The seasonal series are calculated by averaging the monthly σ series. The constant σ value of 4.2 °C is also marked (black dashed line) for direct comparison to the new parameter.

Title Page

Abstract

Introduction

Conclusions

References

Tables

Figures

◀

▶

◀

▶

Back

Close

Full Screen / Esc

Printer-friendly Version

Interactive Discussion



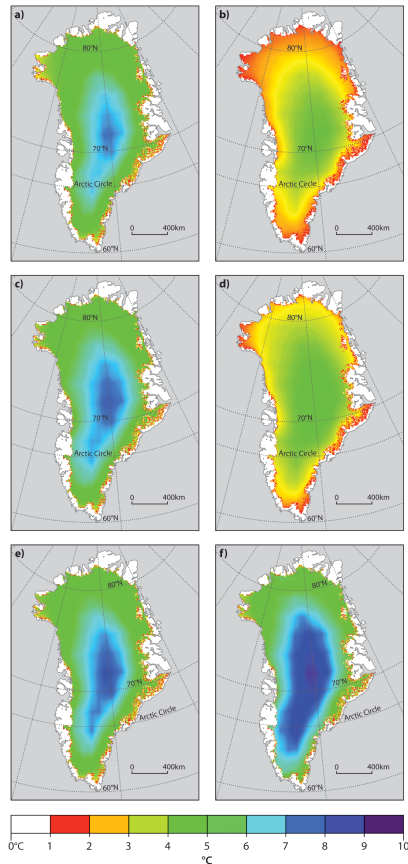


Figure 6. (a) Annual, (b) July, (c) spring, (d) summer, (e) autumn and (f) winter time averaged spatial plots of σ from 1870–2013 inclusive calculated from monthly 2 m air temperatures that have been downscaled, corrected, scaled and corrected for breakpoints.

A new spatially and temporally variable sigma parameter in degree-day melt

A. E. Jowett et al.

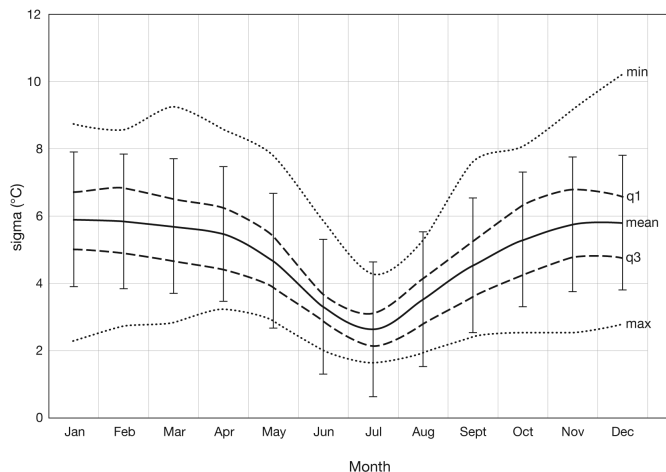


Figure 7. Mean σ for each month (solid line) calculated by averaging the monthly ice sheet averaged σ series for 1870–2013 with standard error bars. Minimum and maximum σ (dotted lines) show the largest and smallest ice sheet average σ for each month. Dashed lines indicate the 25 and 75 % quartiles of ice sheet average σ for each month, showing where 50 % of σ values lie. The seasonal cycle in σ and the spread of values about the mean is clear, along with how this changes over the course of the year.

[Title Page](#)[Abstract](#)[Introduction](#)[Conclusions](#)[References](#)[Tables](#)[Figures](#)[◀](#)[▶](#)[◀](#)[▶](#)[Back](#)[Close](#)[Full Screen / Esc](#)[Printer-friendly Version](#)[Interactive Discussion](#)

A new spatially and temporally variable sigma parameter in degree-day melt

A. E. Jowett et al.

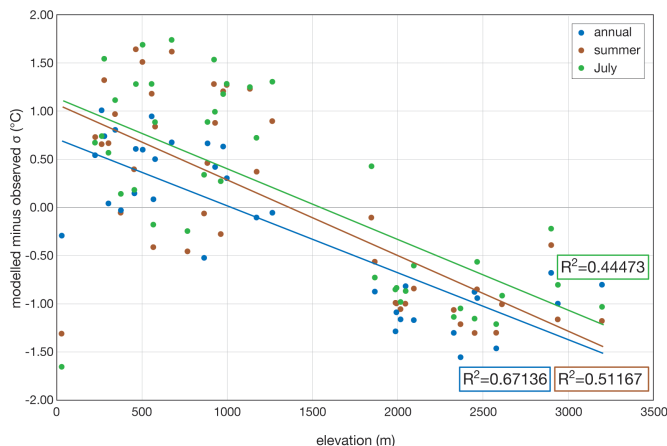


Figure 9. Annual, summer and July difference between modelled and observed σ correlated against elevation, with trend lines and corresponding R^2 values. The ELA is taken to be around 1500 m where there is a systematic shift in the sign of the bias. Where there is a positive difference this indicates the model parameter overestimates σ and where the difference is negative, the model parameter is underestimating σ compared to the observations.

[Title Page](#)[Abstract](#)[Introduction](#)[Conclusions](#)[References](#)[Tables](#)[Figures](#)[◀](#)[▶](#)[◀](#)[▶](#)[Back](#)[Close](#)[Full Screen / Esc](#)[Printer-friendly Version](#)[Interactive Discussion](#)

A new spatially and temporally variable sigma parameter in degree-day melt

A. E. Jowett et al.

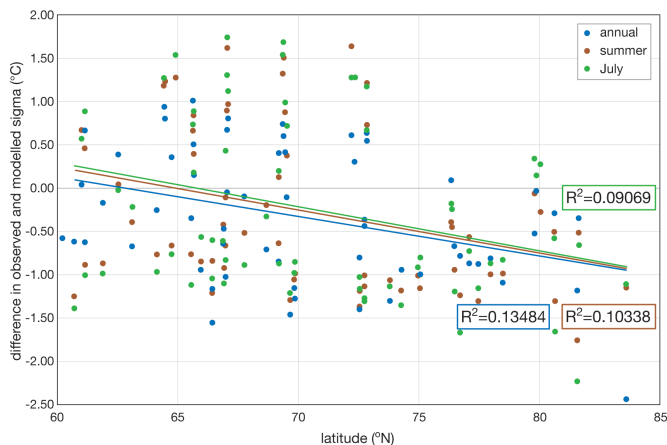


Figure 10. Correlation of the annual, summer and July difference in observed and modelled σ against latitude with trend lines and corresponding R^2 values. The latitude is displayed in decimal degrees to 3 d.p. owing to the latitude of the AWS used in validation.

Title Page

Abstract

Introduction

Conclusions

References

Tables

Figures

◀

▶

◀

▶

Back

Close

Full Screen / Esc

Printer-friendly Version

Interactive Discussion



A new spatially and temporally variable sigma parameter in degree-day melt

A. E. Jowett et al.

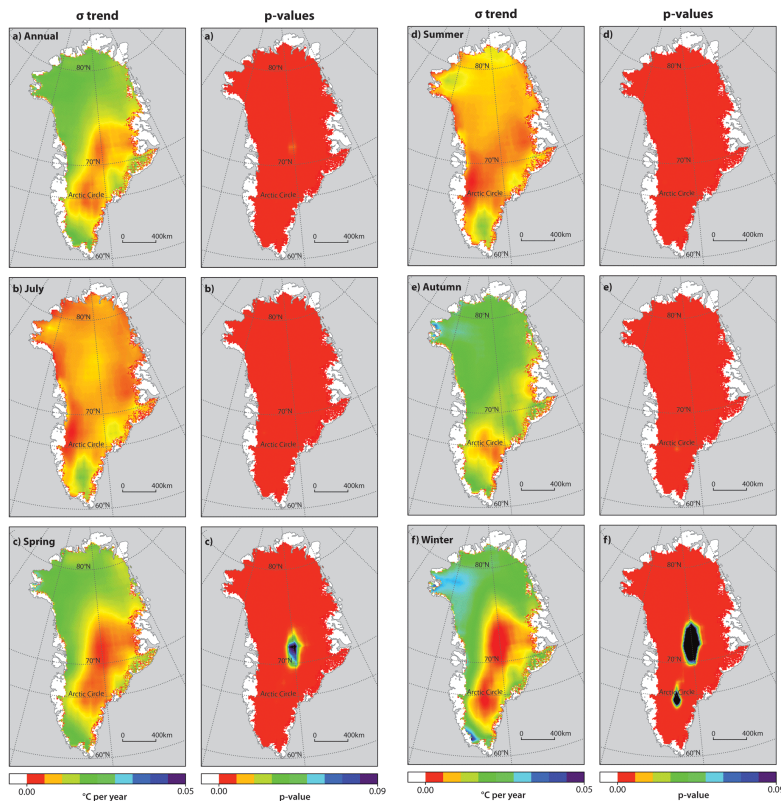


Figure 11. The left hand plots show the rate of change in σ per year from 1870–2013 (σ trend) for each pixel on the ice sheet at the **(a)** annual, **(b)** July, **(c)** spring, **(d)** summer, **(e)** autumn and **(f)** winter scales. The right hand plots show the corresponding statistical significance (p values) to indicate the statistical significance of this rate of change. Values of 0.05 or less (red to green) are statistically significant at the 95 % level.

[Title Page](#)
[Abstract](#)
[Introduction](#)
[Conclusions](#)
[References](#)
[Tables](#)
[Figures](#)
[Back](#)
[Close](#)
[Full Screen / Esc](#)
[Printer-friendly Version](#)
[Interactive Discussion](#)

A new spatially and temporally variable sigma parameter in degree-day melt

A. E. Jowett et al.

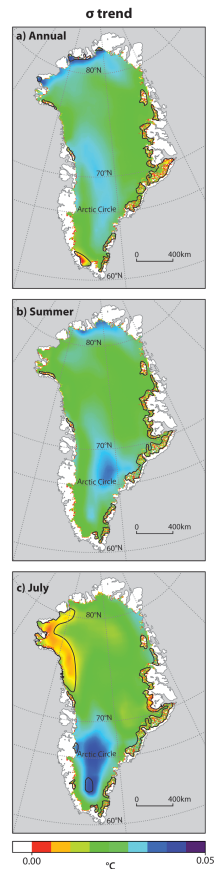


Figure 12. (a) Annual, (b) summer and (c) July sigma trend for the shorter time period 1990–2013. This captures the period of recent change across the GrIS. The areas outlined in black indicate the regions of the ice sheet where these trends are statistically significant at the 95 % level.

A new spatially and temporally variable sigma parameter in degree-day melt

A. E. Jowett et al.

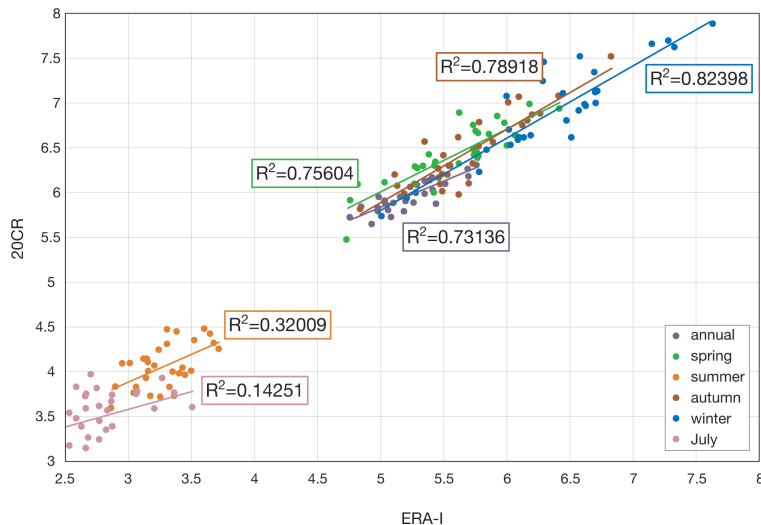


Figure 13. Correlation of ice sheet and time averaged σ calculated from ERA-I and 20CR for the overlap period 1979–2008. The trend lines and corresponding correlation coefficients are displayed for the four seasons, annual and July periods.

Title Page

Abstract

Introduction

Conclusions

References

Tables

Figures

◀

▶

◀

▶

Back

Close

Full Screen / Esc

Printer-friendly Version

Interactive Discussion



A new spatially and temporally variable sigma parameter in degree-day melt

A. E. Jowett et al.

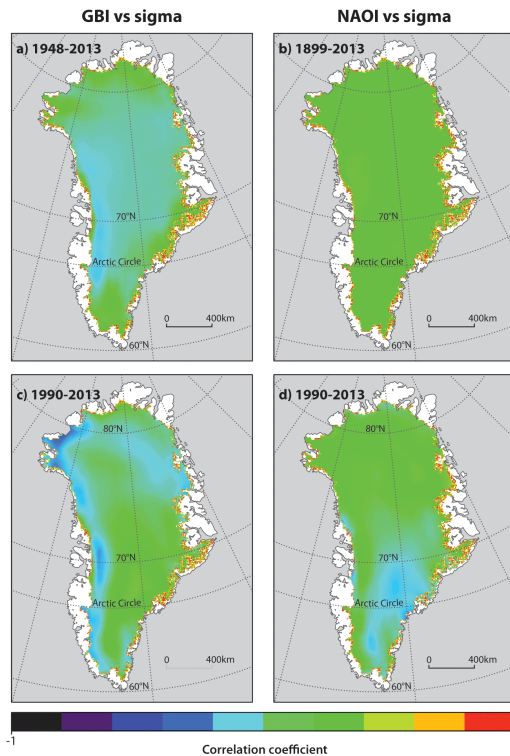


Figure 14. Correlation coefficients of summer NAOI vs. σ from (a) 1899–2013 (b) 1990–2013, and summer GBI vs. σ from (c) 1948–2013 and (d) 1990–2013.

[Title Page](#)
[Abstract](#)
[Introduction](#)
[Conclusions](#)
[References](#)
[Tables](#)
[Figures](#)
[Back](#)
[Close](#)
[Full Screen / Esc](#)
[Printer-friendly Version](#)
[Interactive Discussion](#)